A cluster of familial Creutzfeldt–Jakob disease mutations recapitulate conserved residues in Doppel: a case of molecular mimicry?

Peter Mastrangelo[a], Louise Serpell[d], Tim Dafforn[d], Arthur Lesk[d], Paul Fraser[a,b], David Westaway[a,c,e,*]

[a] *Centre for Research in Neurodegenerative Diseases, University of Toronto, Tanz Neuroscience Building, 6 Queen's Park Crescent West, Toronto, ON, Canada M5S 3H2*
[b] *Department of Medical Biophysics, University of Toronto, Toronto, ON, Canada M5S 3H2*
[c] *Laboratory Medicine and Pathobiology, University of Toronto, Toronto, ON, Canada M5S 3H2*
[d] *University of Cambridge, Structural Medicine Unit, Cambridge Institute for Medical Research, Hills Road, Cambridge CB2 2XY, UK*
[e] *University of Toronto, Centre for Research in Neurodegenerative Diseases, Tanz Neuroscience Building, 6 Queen's Park Crescent West, Toronto, ON, Canada M5S 3H2*

Received 6 September 2002; revised 2 October 2002; accepted 4 October 2002

First published online 1 November 2002

Edited by Thomas L. James

Abstract **Intrachromosomal deletions linking Dpl expression to the PrP promoter produce cerebellar degeneration that can be abrogated by the introduction of wild-type PrP transgenes. Since Dpl-like truncated forms of PrP are neuropathogenic in mice and likewise counterbalanced by expression of PrP^C we asked whether naturally occurring mutant forms of human PrP have Dpl-like attributes. Five *PRNP* missense mutations causing familial Creutzfeldt–Jakob disease (F-CJD) map to a helical region found in both PrP^C and Dpl and result in amino acids identical to conserved residues in Dpl. These F-CJD alleles may cause mutant PrP to become a weak mimetic of Dpl structure and/or function.**

Key words: Paralog cross-talk; Prion; Molecular mimicry

1. Introduction

The prion protein gene encodes a precursor to PrP^{Sc}, the major structural component of prions. Prions are infectious pathogens causing a number of disorders including scrapie and BSE. Prion diseases manifest with diverse neuropathologies that may include spongiform degeneration, deposition of extracellular amyloid deposits, and apoptosis [1–4]. Missense mutations in the human *Prnp* gene cause inherited diseases such as familial Creutzfeldt–Jakob Disease (F-CJD), Gerstmann–Sträussler Scheinker syndrome (GSS), and fatal familial insomnia (FFI) [5]. *Prnp* encodes a protein denoted PrP^C and in prion infections, PrP^C is converted to PrP^{Sc} by templated refolding.

Although many mutations cause familial prion disease it is not possible to predict a priori which missense mutations will lead to a particular clinico-pathological phenotype. F-CJD is a case in point. Although *PRNP* mutations were assumed to cause thermodynamic destabilization of PrP^C, F-CJD mutations have only subtle effects upon the thermal melting profiles of recombinant proteins [6,7]. Expressed in transfected rodent cells, F-CJD alleles of *Prnp* neither engender bona fide protease-resistant PrP^{Sc} nor prion infectivity [8–11] and transgenic mice expressing the E200K mutation do not develop spontaneous neuropathology or prion infectivity [11,12]. These observations have led to the suggestion of pathogenicity from altered ligand binding or interactions with membrane components [13].

Doppel (Dpl) is a recently identified prion protein paralog that, like PrP^C, is GPI-anchored and has three α-helices. Dpl, however, lacks the octapeptide repeat motifs present in PrP and is unlikely to undergo conformational remodeling to a protease-resistant form, or to facilitate remodeling of PrP^C [14–17]. Expression of Dpl in CNS neurons causes cerebellar cell death and vacuolar change in white matter tracts but this pathology is attenuated by expression of wild-type (wt) PrP [18–20], presumably reflecting competition between the activities of the two proteins. Remarkably, some mutant forms of mouse PrP (PrPΔ32-121 and PrPΔ32-134) resembling Dpl also cause ataxia marked by loss of Purkinje cells and apoptosis of cerebellar granule cells. Like Dpl-associated ataxia, this is prevented by addition of wt PrP transgenes [21,22]. These observations led us to ask whether any human *PRNP* mutations are pathogenic by virtue of acquiring Dpl-like characteristics. In this report we examine the structural contexts of pathogenic *PRNP* mutations. In most cases the mutations causing one variety of familial prion disease introduce residues that are conserved in Dpl into PrP. Molecular dynamics calculations, although no substitute for experimental structures, suggest that mutations that introduce Dpl-like features into the sequences may introduce Dpl-like features into the structures.

2. Materials and methods

Experimental structures of recombinant wt PrP, E200K PrP and mouse Dpl were available from the Protein Data Bank (entries 1QLX, 1F07 and 1I17, respectively) (http://www.rcsb.org/pdb).

Molecular mechanics study of Dpl was carried out using the published nuclear magnetic resonance (NMR) structure [14]. Mutations were made in the PrP sequence using Insight II 98.0 (MSI, San Diego, CA, USA). Side chain conformations for the mutated residues were selected by examination of common rotomers from a side chain ro-

*Corresponding author. Fax: (1)-416-978 1878.
E-mail address: david.westaway@utoronto.ca (D. Westaway).

0014-5793/02/$22.00
PII: S0014-5793(02)03614-1

tomer library. The rotomer producing the least steric clashes was selected in each case. The structure was then soaked in an 8 Å layer of water and the charges on the protein set to values consistent with an environmental pH of 7.0. Each structure was parameterized using the CVFF force field [23] and energy minimized. The minimization routine contained four sequential steps to allow bad steric contacts to be resolved without unwanted distortions to the rest of the structure. (1) All hydrogens were minimized using a steepest descents minimizer until the maximum derivative was less than 0.0010000 kcal/Å; (2) all side chains were minimized using a steepest descents minimizer while the backbone was tethered with a force constant of 1000.0 kcal/Å^2 until the maximum derivative was less than 0.50000 kcal/Å; and (3) step 2 was repeated twice more using the conjugate gradients minimizer while reducing the force constant to 100 kcal/Å^2 and 0, respectively. The structures were then subjected to 24 ps of molecular dynamics simulation at 300 K. All molecular mechanics studies were carried out using a cut-off distance of 30 Å for the non-bond interaction calculation. These data were then used for structural alignment (see main text).

Root mean square deviations (RMSDs) were calculated by a structural alignment procedure that seeks to determine a maximal common well-fitting substructure [24]. The method first tests all pairs of short regions, adaptively, and then combines them to determine the largest coherent substructure that retains the same topology. The calculations are an adaptation of the methods described in Chothia and Lesk [25].

3. Results

3.1. F-CJD missense mutations recapitulate Dpl residues

Our objective was to test the hypothesis that some mutant forms of PrP might be pathogenic by virtue of acquiring Dpl-like properties. While primitive 'PrP-like' genes have been reported in a variety of vertebrates [26,27], it is unclear whether these organisms have prion gene complexes encoding functional homologs of PrP and Dpl. Consequently we focussed upon mammals that both satisfy this criterion and are susceptible to prion infections. A structure-based alignment of PrP and Dpl sequences was used to study the relationship between mutations in the human *Prnp* gene (*PRNP*) and the *Prnd* gene encoding Dpl (Fig. 1). Our starting data-set comprised all reported prion mutations lying within the coding regions of the PrP and Dpl (i.e. excluding sequences and mutations lying within the N- and C-terminal signal peptides that are removed during protein maturation). Cases defined by a single patient or where neuropathological analysis was missing or inconclusive were excluded. In the case of GSS it was not possible to undertake meaningful analyses for the causative P102L, P105L and A117V mutations as these are located within an area of PrP that has no cognate in Dpl [16]. Since the remaining GSS mutations (G131V, H178R, F198S, D202N, Q212P and Q217R) do not result in the creation of amino acid residues that are also conserved in Dpl, the hypothesis that GSS *PRNP* alleles result in PrP^C molecules more Dpl-like than wt PrP^C was rejected. Similarly, although stop codon mutations at positions 145 or 160 are observed in conjunction with neurodegenerative syndromes [28,29], these mutant forms of PrP terminate before the α-helical region shared between PrP and Dpl, and were also not considered further. On the other hand, a relationship was noted for five F-CJD mutations (V180I, E196K, E200K, V210I, and E211Q: Table 1).

In all cases the wt residue affected by these mutations is absolutely conserved between the PrP gene sequences presented in Fig. 1, as well as a compilation from a total of 46 mammals [30]. Of these, V180I, E196K, E200K and E211Q result in amino acid changes that are exactly conserved in human Dpl, while V210I involves an isoleucine conserved in mouse, cow, sheep and rat Dpl proteins (Fig. 1). The sixth well-studied F-CJD mutation D178N (more commonly found in association with FFI when in *cis* to the Met 129 polymorphism) is represented by a glycine in Dpl and does not fit the pattern of conservation.

Assignment of Dpl residues analogous to the six human mutations was not based solely upon sequence alignment, but also upon experimentally determined NMR structures of recombinant PrP [31] and Dpl [14] (Fig. 1). Dpl residues equivalent to the D178N and V180I mutations are absolutely positioned by invariant conserved residues at V176 (human PrP numbering scheme), C179, N181, and T183. E200, mutated to lysine in the E200K F-CJD allele, is the N-terminal residue of helix C in both PrP and Dpl, while V210 and E211, mutated to I and Q respectively in F-CJD, are bracketed on the N-terminal side by an invariant R208 residue and on the C-terminal side by C214. The sixth instance comprises E196, which is mutated to lysine in F-CJD and is positioned on the C-terminal side by the aforementioned E200 residue.

Table 1
F-CJD mutations mimic features of Dpl

PRNP mutations[a]	Amino acid residue comparisons		PrP/Dpl structural comparisons based upon molecular mechanics simulation[e]			
	Analogous residue in HuDpl[b]	Other possible residues[d]	Allele modeled	Residues superimposed	RMSD per atom	Identical residues in alignment
Wild type	n.a.[c]	n.a.	Wild type	61	3.50	13
D178N (11)	G(S)	A, E, G, H, Y, V	178N	61	3.45	13
V180I (4)	I (I)	A, D, G, L, F	180I	59	2.26	12
E196K (3)	K(K)	A, D, E, G, Q, V, Stop	196K	71	2.38	15
E200K (63)	K(K)	A, D, E, G, V, Stop	200K	66	2.18	18
			200K NMR structure	**68**	**1.87**	**15**
V210I (5)	V(I)	n.a.	210I	65	2.13	17
E211Q (3)	Q(K)	A, D, E, G, K, V, Stop	211Q	71	2.23	12

[a]Number of reported cases in parentheses. See [5,46] for references to the individual mutations. Mutations defined by a single case or where neuropathological analysis was missing or inconclusive were not considered further. These include T188R, T188K, T188A, V203I, R208H and M232R (see also main text).
[b]Dpl consensus shown in brackets.
[c]n.a., not applicable.
[d]Alternative missense and nonsense substitutions arising from hypothetical single nucleotide changes in the relevant codon.

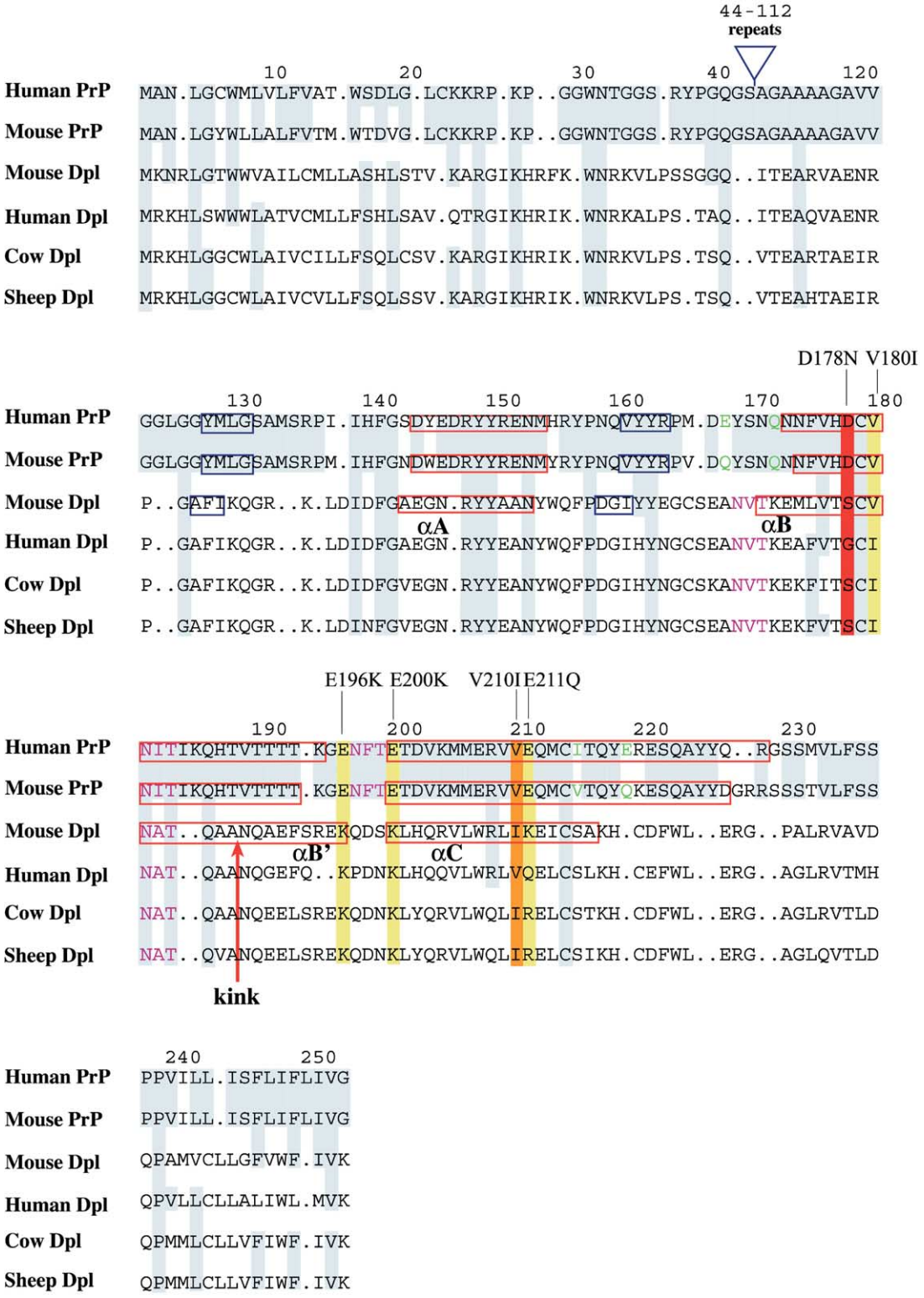

Fig. 1. Structural alignment of human and mouse PrP with mouse, human, cow and sheep Dpl. The alignment of mouse PrP with mouse Dpl is based on that of Mo et al. [14]. Residues identical to human PrP are highlighted in light blue. α-Helical regions (αA, αB, αB′ and αC) are indicated by red boxes and β-sheet by blue boxes. A kink in Dpl αB helix is indicated by a red arrow. Different CJD mutations under consideration are indicated above the corresponding residues in human PrP. Yellow bars indicate a residue that changes in human PrP to the corresponding CJD mutant residue in human Dpl, orange bars indicate a partial correspondence, and a red bar signifies no correspondence. The numbering is with respect to human PrP. A region containing the octarepeats that has no equivalent in Dpl has been removed from this alignment for clarity. Green residues represent the discontinuous epitope that defines the binding site for 'protein X' [36]. Consensus glycosylation sites are in purple.

3.2. PRNP and PRND gene sequences

To address a possible relationship arising as a trivial consequence of gene sequence or codon usage we inspected nucleotide sequences of the respective genes. Attempts to perform pair-wise 'BLAST' alignments of the complete open reading frames of the human PrP (*PRNP*) and Dpl (*PRND*) genes failed to reveal nucleotide homology (BLAST 2.2.1: http://www.ncbi.nlm.nih.gov/blast), as noted previously [16]. A similar result was obtained when restricting the analysis to DNA sequences encoding the αB-loop-αC regions and αB/B′-loop-αC regions of *PRNP* and *PRND*, respectively. To assess 'micro' sequence homology occurring in restricted polynucleotide tracts, sequences were compiled for *PRNP* codons prone to F-CJD mutations, their flanking 5′ and 3′ codons, and the corresponding *PRND* nucleotides (data not shown). Failure to define a constant relationship between the nucleotide codons of V180, E196, E200 and E211 and their equivalents in the human Dpl gene lead us to consider the properties of the respective proteins.

3.3. Properties of E196K, E200K, and E211Q F-CJD mutations

These F-CJD mutants all affect (wt) glutamic acid residues in human PrP, are perfect matches to the analogous human Dpl residues, and result in a change to a basic residue. All are closely juxtaposed and face upwards (E200 and E211) or outwards (E196) from the plane of the αB-loop-αC sub-domain [13,31]. Residues with the analogous positions in mouse Dpl (i.e. Dpl residues K125, K129 and K140) adopt similar dispositions with respect to the plane of the αB′-loop-αC subdomain (Fig. 2). To assess further similarities between Dpl and mutant PrP^{C} the NMR solution structure determined for recombinant human E200K PrP [13] (RMSD = 0.4–0.7 Å) was overlaid on the Dpl NMR structure. Overlay yielded an RMSD of 1.87 Å for the E200K PrP–Dpl comparison versus 3.50 Å for the wt PrP–Dpl comparison, emphasizing the similarity between the E200K PrP and wt Dpl [32](bold text in Table 1). Since NMR structures do not exist for the E196K and E211Q proteins we modeled these mutations with molecular dynamics simulation using Insight II 98.0 (MSI), starting with the wt human PrP structure [31]. This modeling paradigm has been validated experimentally [33]. We modeled E200K in the same fashion as an internal control. Data presented in Table 1 give the total number of superposable Cα atoms and the number of superposed residues that contain identical amino acids [32]. RMSD values of the superimposable Cα atoms of the E196K (2.36 Å), E200K (2.18 Å) and E211Q (2.23 Å) proteins are lower than wt PrP (3.5 Å), indicating that these structures are more Dpl-like. The RMSD value for the modeled E200K–Dpl comparison is larger than that for the experimentally determined structure E200K–Dpl comparison (2.18 Å versus 1.87 Å), suggesting that these molecular dynamics analyses may underestimate similarities with Dpl.

3.4. Properties of the V180I and V210I F-CJD mutations

V180I and V210I are conservative changes in residues almost directly opposite one another on the inside faces of αB and αC within PrP′s hydrophobic core [34]. When modeled by molecular mechanics on the wt HuPrP NMR these analyses revealed a substantial change in the RMSD values for the V180I (2.26 Å) and V210I (2.13 Å) proteins compared to wt HuPrP (3.5 Å), an alteration again in the direction of the Dpl structure. Considered collectively, averaged RMSD values per atom for V180I, E196K, E200K, V210I and E211Q were 2.24 ± 0.09 Å, versus 3.50 and 3.45 Å for wt PrP and D178N PrP, respectively. The data also showed a tendency for a greater number of superimposed residues and identical residues in the alignment when again considering V180I, E196K, E200K, V210I and E211Q mutant proteins versus wt PrP and D178N PrP (Table 1).

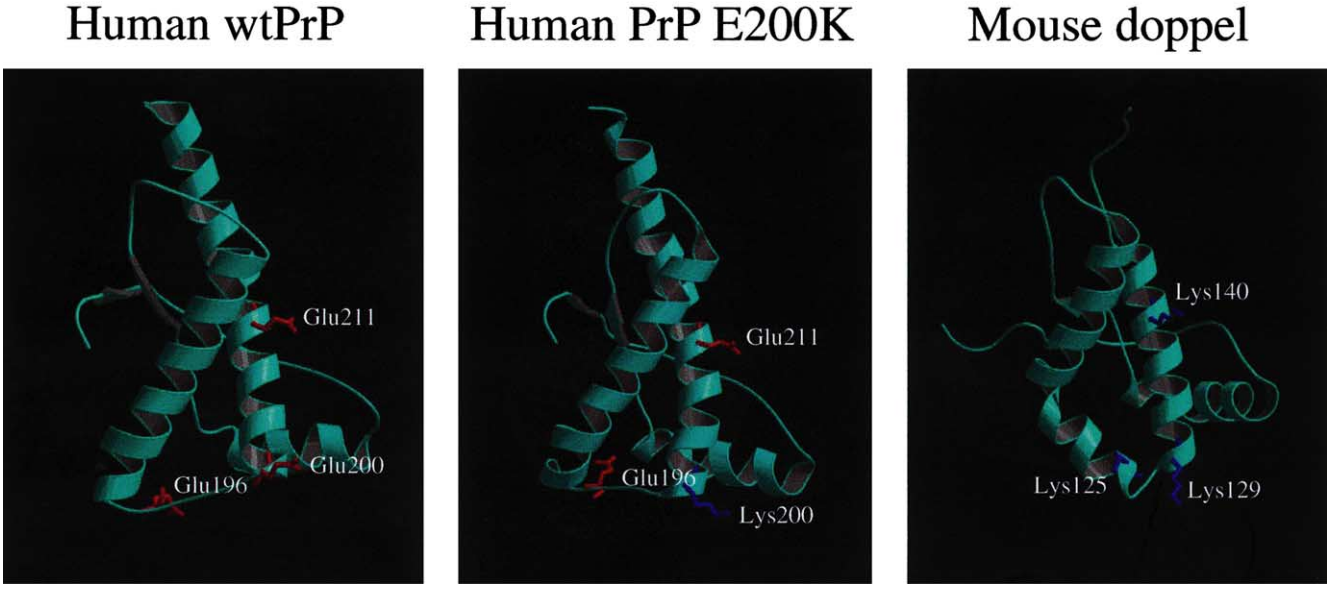

Fig. 2. 3D models of human PrP, human PrP E200K and mouse Dpl. The protein backbone and structural motifs (α-helices and β-sheets) are shown in light blue and gray. Selected residues are represented as 'ball-and-stick' molecules: red for acidic and blue for basic. The residues under consideration are Glu196, Glu200 and Glu211 for human PrP; Glu196, Lys200 and Glu211 for human PrP E200K; and Lys125, Lys129 and Lys140 for mouse Dpl. The models are based on NMR coordinates obtained from the literature [13,14,31]. Images were generated with MOLSCRIPT [45].

3.5. F-CJD mutations and protein X

One explanation for pathogenic effect of F-CJD mutations is that they occur in a binding site for interactions with other macromolecules. Since the notion of a binding site within the α-helical domain of PrP has been proposed in the context of a hypothetical protein X, the locations of F-CJD mutations were compared with those of residues deemed important for protein X binding [35,36]. The two sets of residues do not overlap (Fig. 1, shown in green).

4. Discussion

We describe a relationship between a cluster of F-CJD mutations and the structure of the Dpl protein [16], whereas no similar trend was noted in a compilation of GSS mutations. In four instances of F-CJD mutations perfectly recapitulate conserved residues in the α-helical domain of human Dpl. If this correlation holds true we would predict that 'new' F-CJD missense alleles will map to PrP^C's αB-loop-αC region and result in Dpl-like residues. Specifically, we would predict that mutations M205V, M206L, V209L arising from single nucleotide substitutions (as well as T188A, currently defined by one case) will cause F-CJD. At this stage, the D187N mutation comprises the clear exception to the general rule. Whether the D178N mutation causes CJD by a distinct mechanism, perhaps related to an involvement of residue 178 in salt bridge [37] with residues Asp178 and Arg164 (which have no exact equivalent in Dpl) remains to be established. While N-terminal insertions of *PRNP* also cause F-CJD, it is interesting to note that interactions between the N-terminus of PrP and a region of interest here, helixB, have been documented by previous NMR analysis [38].

4.1. Mutational and evolutionary considerations

In the context of recent gene duplications one might imagine that parallelism could emerge between the pattern of mutations in one gene versus the DNA sequence of the adjacent gene. However, standard 'BLAST' algorithms failed to reveal homology between mouse *Prnp* and *Prnd*. Even using an artificial alignment considering the affected codon plus one 5′ and one 3′ codon no consistent relationship was noted between nucleotide sequences of the five selected F-CJD mutations and the *PRND* nucleotide sequence (data not shown).

4.2. Mechanisms involving protein structure and function

End-stage F-CJD is marked by accumulation of protease-resistant PrP and infectious prion titer [35,39–42], observations implying conformational reorganization of PrP^C. Whether this PrP^{Sc} arises from thermodynamic destabilization or from a cell biological mechanism (e.g. altered metabolism or trafficking) is unclear, and current attempts to 'model' F-CJD, and hence provide an assay to test pathogenic mechanisms, have not been successful.

The correlation between F-CJD mutations and conserved Dpl residues described herein suggests a new possibility, namely that the mutations in this disease erode a boundary between certain PrP^C- and Dpl-associated functions. This notion is compatible with two studies dealing with the expression and copy-number of the wt *PRNP* allele in F-CJD. Decreased expression of the wt allele has been implicated in disease onset in E200K carriers, perhaps by reducing a protective effect [43] and homozygosity for E200K has been reported to hasten disease onset [44]. These data parallel the protective effect of PrP^C expression upon Dpl-mediated neurotoxicity [18]. Our results suggest that studies to delineate the biochemical activities and binding partners of Dpl and PrP^C, and the role of the cluster of charged residues in PrP′s αB-loop-αC region may provide insight into pathogenesis, as well as cell physiology.

Acknowledgements: We thank Jennifer Griffin for helpful comments. P.M. is a Peterborough-Burgess Fellow of the Alzheimer Society of Ontario and this work was supported by grants to D.W. from the Canadian Institutes of Health Research (MOP363377 and MSC 46763). A.M.L., T.D. and L.C.S. are supported by the Wellcome Trust.

References

[1] Fraser, H. (1993) Br. Med. Bull. 49, 792–809.
[2] Lucassen, P.J., Williams, A., Chung, W.C. and Fraser, H. (1995) Neurosci. Lett. 198, 185–188.
[3] Brown, D., Belichenko, P., Sales, J., Jeffrey, M. and Fraser, J.R. (2001) NeuroReport 12, 179–183.
[4] Jamieson, E., Jeffrey, M., Ironside, J.W. and Fraser, J.R. (2001) NeuroReport 12, 3567–3572.
[5] Parchi, P., Gambetti, P. and Ghetti, B. (1998) in: Progress in Pathology (Kirkham, N. and Lemoine, N.R., Eds.), pp. 39–77, Churchill-Livingstone, Edinburgh.
[6] Swietnicki, W., Petersen, R.B., Gambetti, P. and Surewicz, W.K. (1998) J. Biol. Chem. 273, 31048–31052.
[7] Liemann, S. and Glockshuber, R. (1999) Biochemistry 38, 3258–3267.
[8] Lehmann, S. and Harris, D.A. (1996) J. Biol. Chem. 271, 1633–1637.
[9] Vetrugno, V., Malchow, M., Liu, Q., Marziali, G., Battistini, A. and Pocchiari, M. (1999) Neurosci. Lett. 270, 41–44.
[10] Capellari, S., Parchi, P., Russo, C.M., Sanford, J., Sy, M.S., Gambetti, P. and Petersen, R.B. (2000) Am. J. Pathol. 157, 613–622.
[11] Rosenmann, H., Talmor, G., Halimi, M., Yanai, A., Gabizon, R. and Meiner, Z. (2001) J. Neurochem. 76, 1654–1662.
[12] Telling, G.C., Haga, T., Torchia, M., Tremblay, P., DeArmond, S.J. and Prusiner, S.B. (1996) Genes Dev. 10, 1736–1750.
[13] Zhang, Y., Swietnicki, W., Zagorski, M.G., Surewicz, W.K. and Sonnichsen, F.D. (2000) J. Biol. Chem. 275, 33650–33654.
[14] Mo, H., Moore, R.C., Cohen, F.E., Westaway, D., Prusiner, S.B., Wright, P.E. and Dyson, H.J. (2001) Proc. Natl. Acad. Sci. USA 98, 2352–2357.
[15] Behrens, A., Brandner, S., Genoud, N. and Aguzzi, A. (2001) EMBO Rep. 2, 347–352.
[16] Moore, R. et al. (1999) J. Mol. Biol. 293, 797–817.
[17] Nicholson, E.M., Mo, H., Prusiner, S.B., Cohen, F.E. and Marqusee, S. (2002) J. Mol. Biol. 316, 807–815.
[18] Moore, R. et al. (2001) Proc. Natl. Acad. Sci. USA 98, 15288–15293.
[19] Nishida, N. et al. (1999) Lab. Invest. 79, 689–697.
[20] Rossi, D., Cozzio, A., Flechsig, E., Klein, M.A., Rulicke, T., Aguzzi, A. and Weissmann, C. (2001) EMBO J. 20, 694–702.
[21] Shmerling, D. et al. (1998) Cell 93, 203–214.
[22] Weissmann, C. and Aguzzi, A. (1999) Science 286, 914–915.
[23] Dauber-Osguthorpe, P., Roberts, V.A., Osguthorpe, D.J., Wolff, J., Genest, M. and Hagler, A.T. (1988) Proteins 4, 31–47.
[24] Irving, J.A., Whisstock, J.C. and Lesk, A.M. (2001) Proteins 42, 378–382.
[25] Chothia, C. and Lesk, A.M. (1986) EMBO J. 5, 823–826.
[26] Simonic, T., Duga, S., Strumbo, B., Asselta, R., Ceciliani, F. and Ronchi, S. (2000) FEBS Lett. 469, 33–38.
[27] Strumbo, B., Ronchi, S., Bolis, L.C. and Simonic, T. (2001) FEBS Lett. 508, 170–174.
[28] Ghetti, B. et al. (1996) Proc. Natl. Acad. Sci. USA 93, 744–748.
[29] Finckh, U. et al. (2000) Am. J. Hum. Genet. 66, 110–117.
[30] Wopfner, F., Weidenhofer, G., Schneider, R., von Brunn, A., Gilch, S., Schwarz, T.F., Werner, T. and Schatzl, H.M. (1999) J. Mol. Biol. 289, 1163–1178.

[31] Zahn, R. et al. (2000) Proc. Natl. Acad. Sci. USA 97, 145–150.
[32] Lesk, A.M. (1986) in: Biosequences: Perspectives and User Services in Europe (Saccone, C., Ed.), pp. 23–28, EEC, Brussels.
[33] Dafforn, T.R., Badcoe, I.G., Sessions, R.B., el Hawrani, A.S. and Holbrook, J.J. (1997) Proteins 29, 228–239.
[34] Riek, R., Hornemann, S., Wider, G., Billeter, M., Glockshuber, R. and Wuthrich, K. (1996) Nature 382, 180–183.
[35] Telling, G.C., Scott, M., Mastrianni, J., Gabizon, R., Torchia, M., Cohen, F.E., DeArmond, S.J. and Prusiner, S.B. (1995) Cell 83, 79–90.
[36] Kaneko, K., Zulianello, L., Scott, M., Cooper, C.M., Wallace, A.C., James, T.L., Cohen, F.E. and Prusiner, S.B. (1997) Proc. Natl. Acad. Sci. USA 94, 10069–10074.
[37] Riek, R., Wider, G., Billeter, M., Hornemann, S., Glockshuber, R. and Wuthrich, K. (1998) Proc. Natl. Acad. Sci. USA 95, 11667–11672.
[38] Donne, D. et al. (1997) Proc. Natl. Acad. Sci. USA 94, 13452–13457.
[39] Bockman, J.M., Prusiner, S.B., Tateishi, J. and Kingsbury, D.T. (1987) Ann. Neurol. 21, 589–595.
[40] Brown, P., Gibbs Jr., C.J., Rodgers-Johnson, P., Asher, D.M., Sulima, M.P., Bacote, A., Goldfarb, L.G. and Gajdusek, D.C. (1994) Ann. Neurol. 35, 513–529.
[41] Parchi, P. et al. (1999) Ann. Neurol. 46, 224–233.
[42] Mastrianni, J.A., Capellari, S., Telling, G.C., Han, D., Bosque, P., Prusiner, S.B. and DeArmond, S.J. (2001) Neurology 57, 2198–2205.
[43] Rosenmann, H., Halimi, M., Kahana, I., Biran, I. and Gabizon, R. (1997) Neurology 49, 851–856.
[44] Simon, E.S., Kahana, E., Chapman, J., Treves, T.A., Gabizon, R., Rosenmann, H., Zilber, N. and Korczyn, A.D. (2000) Ann. Neurol. 47, 257–260.
[45] Kraulis, P.J. (1991) J. Appl. Cryst. 24, 946–950.
[46] Prusiner, S.B. and Scott, M.R. (1997) Annu. Rev. Genet. 31, 139–175.